Ordered bicontinuous double diamond structure in block copolymer / homopolymer blends

Hideaki Takagi[a]*, Katsuhiro Yamamoto[b]*, Shigeru Okamoto[b],

[a]*Photon Factory, Institute of Materials Structure Science, High Energy Accelerator Research Organization, 1-1 Oho, Tsukuba, Ibaraki 305-0801, Japan*

[b]*Graduate School of Engineering, Department of Materials Science & Technology, Nagoya Institute of Technology, Gokiso-cho, Showa-ku, Nagoya 466-8555, Japan*

* To whom all correspondence should be addressed Tel./fax: +81-29-864-5299; + 81-52-735-5277.

 E-mail address: takagih@post.kek.jp (H. Takagi), yamamoto.katsuhiro@nitech.ac.jp (K. Yamamoto)

ABSTRACT: The morphologies of the microdomain structures in polystyrene-polyisoprene diblock copolymer (PS-PI) and polyisoprene homopolymer (PI) blends were investigated by small angle X-ray scattering. The PS-PI investigated in the present study has number-average molecular weight M_n = 38,400 g / mol and volume fraction of PI f_{PI} = 0.33, and PI has M_n = 11,400. The weight fraction of added homopolymer was 0.17. We demonstrated that the existence of ordered bicontinuous double diamond (OBDD) structure was explicitly identified in PS-PI / PI blend by scattering method. It was confirmed that OBDD microdomain changed to gyroid (Gyr) when the sample was heated, and the order-order transition between OBDD and Gyr thermo-reversibly occurred. The kinetics of the transformation between OBDD and Gyr was also investigated. In this study, the intermediate structure during the transition between OBDD and Gyr was not observed. A comparison between the rates of transformation revealed that the rate of the OBDD to Gyr transformation is faster than that of the Gyr to OBDD.

INTRODUCTION

The bicontinuous structures observed in block copolymers have captivated researchers due to various technological applications, such as hybrid solar cells, photonic crystals, optical metamaterials, etc [1,2]. It has been reported that there are the two types of bicontinuous structure, gyroid (Gyr) and *Fddd*, in block copolymer melts; Gyr is constructed by 3-fold nodes connected with *Ia3d* symmetry [3], and *Fddd* is noncubic single network in an orthorhombic unit cell, and constructed by 3-fold nodes [4]. Recently, ordered bicontinuous double diamond (OBDD) which is constructed by 4-fold nodes connected with *Pn3m* symmetry was discovered in syndiotactic polypropylene-polystyrene (sPP-PS) block copolymer [5]. In this system, OBDD appeared in the lower temperature side, while Gyr was observed in higher temperature. It was reported that the transformation between the OBDD and Gyr was thermo-reversible. The reason why the OBDD in sPP-PS was thermodynamically stabilized was that the higher packing frustration in nodes was relaxed due to the existence of the population of helical segments of syndiotactic polypropylene.

It is interesting to look back in the history of the discovery of bicontinuous structure in block copolymers. For more detailed explanation of the history, the reader can refer to the review [1]. Here, we summarize briefly as follows. In 1986, OBDD was first observed in polystyrene-polyisoprene (PS-PI) starblock copolymers [6]. Thereafter, OBDD also appeared in diblock copolymer [7] and diblock copolymer / homopolymer blends [8,9]. A number of theoretical studies showed that OBDD was never predicted to be an equilibrium structure [9,10]. Eventually, from rigorous experimental analysis using small angle scattering techniques, the bicontinuous structures reported previously were not OBDD but Gyr in linear diblock copolymers [11]. Some of experimental results in which observed bicontinuous structure was reported as OBDD had been re-examined and classified as Gyr in block copolymer / homopolymer blends [12,13] and starblock copolymers [14]. Since the OBDD mesostructure resembles the Gyr morphology, the transmission electron microscopy (TEM) images obtained from Gyr closely mirror those expected from the OBDD. Therefore, the Gyr morphology was misidentified as OBDD [1].

It is well known that the packing frustration of chain segments exists inside a bicontinuous node [15,16]. Packing frustration is further increased in a node of OBDD as compared with Gyr, since minority chain segments have to be stretched more to fill the space at the center of the four-connector in OBDD as compared with that of three-connector in Gyr [5]. Thus, it is considered that OBDD could not be formed in a diblock copolymer. However, in the case of a block copolymer and homopolymer blend, theoretical researchers predicted that OBDD network would be stable for some blend compositions [17,18]. As mentioned above, some of experimental research groups had re-examined their past work, but the others did not report what they had observed actually in their study. At least, to the best of our knowledge, there are no reports that the observed morphologies had been identified as OBDD in block copolymers and/or block copolymer/homopolymer blend except for sPP-PS having a specific helical conformation.

Although it is difficult to distinguish between OBDD and Gyr using TEM, the difference between those structures can be easily identified from diffraction peak positions obtained by scattering method. In this paper, first, we demonstrated that the OBDD structure was actually observed in block copolymer (PS-PI) / homopolymer (PI) blends by scattering technique. Second, we investigated the kinetic behavior of phase transitions between OBDD to Gyr phases.

EXPERIMENTAL SECTION

Polystyrene-polyisoprene (PS-PI) diblock copolymer was synthesized by anionic polymerization under vacuum. The isoprene monomer in toluene was first polymerized at room temperature for 24 hours using *sec*-butyllithium as the initiator. After completing the polymerization of isoprene monomer, a small amount of polyisoprene / toluene solution was transferred into a glass tube attached with the reaction container under vacuum. The glass tube was sealed off and the content was obtained to evaluate molecular weight of the precursor polyisoprene. Then, styrene monomer was added through another glass tube connected with the reaction container in order to synthesize the block copolymer at room temperature. The number -average molecular weight (M_n) and its heterogeneous

4

index (M_w/M_n) were determined by size exclusion chromatography (SEC) using PI standards. The M_n of the synthesized PS-PI was 38,400, and the M_w / M_n was 1.03. The volume fraction of PI (f_{PI}) was calculated from ^{1}H-NMR (f_{PI} = 0.35). The polyisoprene homopolymer (PI) was also synthesized by anionic polymerization under vacuum (M_n = 11,400 and M_w / M_n = 1.02). The total degree of polymerization (N) is defined by following equation

$$N = \frac{v_{PS}N_{PS} + v_{PI}N_{PI}}{\sqrt{v_{PS}v_{PI}}} \qquad (1)$$

where v_{PS} and v_{PI} are the molar volume and taken to be 75.6 and 99.0 cm^3/mol, respectively [19]. N_{PS} and N_{PI} are the degree of polymerization of PS and PI, respectively. The ratio (a) of homopolymer chain length (N_h) to total chain length of the block copolymer (N_{block}) is defined as $a = N_h/N_{block}$. The a of the PS-PI / PI blend used in this study was 0.51.

Blend sample was prepared as follows: after dissolving a predetermined amount of PS-PI and PI into toluene with total polymer concentration of ca. 5 wt%, the solvent was slowly evaporated for a few weeks at ambient temperature. The weight fraction of added PI was 0.17. After complete removal of the solvent, the cast sample was dried in vacuum for a long time (at least 48 hours) at room temperature. The film was annealed at 120 °C in vacuum oven for 24 h.

The small angle X-ray scattering (SAXS) measurements with synchrotron radiation were conducted at the beamline BL15A in Photon Factory (PF) of High Energy Accelerator Research Organization in Tukuba, Japan (KEK) and at the beamline BL40B2 in SPring-8 in Hyogo. A charge-coupled device (C7300) with an image intensifier (Hamamatsu Photonics Co., Ltd.) (II-CCD at PF) and imaging plate (BAS2500 at PF and R-Axis IV at SPring8) were used as a detector, and the detector was set at a position of 230 cm apart from sample position. The energy of X-ray was 8.3 keV. Collagen (chicken tendon) was used as a standard specimen to calibrate SAXS detectors. The scattering intensities were corrected for background scattering and sample absorption. The magnitude of scattering vector (q) is given by

$$q = \frac{4p}{l} \sin \frac{q}{2} \qquad (2)$$

where l is the wavelength of the X-ray and q is the scattering angle. The sample temperature was controlled using Linkam LK-600M (Japan Hightech). The morphology of neat PS-PI was determined from SAXS. The neat sample showed the order-order transition between hexagonally packed cylinders and Gyr around 150 °C.

RESULTS AND DISCUSSION

Fig. 1 shows SAXS profiles of the blend sample in heating process. The relative diffraction peak positions obtained at 140 °C (bottom profile) were 1 : 1.22 : 1.41 : 1.73 : 1.99 : 2.09 as marked by thin arrows. Here, theoretical relative q-peak positions for OBDD, Gyr and *Fddd* are shown in table 1 in comparison with observed ones. Since the observed SAXS profile at 140 °C had the second order peak around 1.22, it was not ascribed to Gyr. The observed third diffraction peak was not coincidence with that of *Fddd* structure (1.55), but consistence with the second order peak of OBDD (1.41). Additionally the fifth peak (1.81) and sixth peak (1.95) of *Fddd* were also not observed. The structure observed at 140 °C was not *Fddd*. The relative peak positions (1.99 and 2.09) obtained in our blend sample were almost in good agreement with fifth (2) and sixth (2.12) of OBDD, respectively. Therefore, we ruled out the formation of both *Fddd* and Gyr structures.
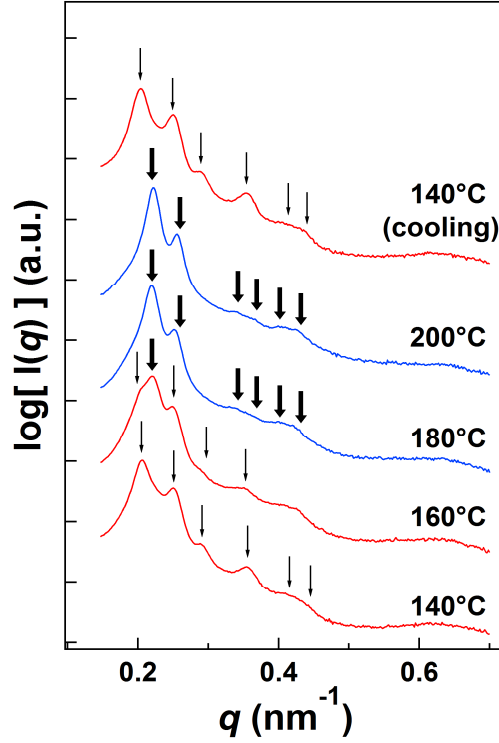
Fig. 1. SAXS profiles of PS-PI / PI blend during heating process. SAXS profile after cooling from 200 °C to 140 °C is also shown (top profile). Thin arrows show scattering peaks from OBDD structure, and thick arrows represent scattering peaks from Gyr structure.

Table 1. Calculated relative peak positions of OBDD, Gyr, *Fddd* and observed relative peak positions.

	1st	2nd	3rd	4th	5th	6th
observed	1	1.22	1.41	1.73	1.99	2.09
OBDD	1	1.22	1.41	1.73	2	2.12
Gyr	1	1.15	1.53	1.63	1.83	1.91
Fddd	1	1.22	1.55	1.72	1.81	1.94

We calculated the theoretical scattering curve by assuming *Pn3m* space group symmetry to compare the experimental profile with theoretical one [20]. The scattered intensity $I(q)$ is given by

$$I(q) = (b_1 - b_2)^2 r_N P(q) S(q) \qquad (3)$$

b_1 and b_2 are scattering length densities of the particles and the surrounding matrix, r_N is the number

density of the particles, and $P(q)$ is the form factor. The structure factor $S(q)$ is given by

$$S(q) = 1 + b(q)[Z(q) - 1]G(q) \qquad (4)$$

$b(q) = \langle F(q) \rangle / \langle F^2(q) \rangle$ is the ratio of the squared scattering amplitude, $G(q)$ is the Debye-Waller factor, and $Z(q)$ the lattice factor given by

$$Z(q) = \frac{(2\pi)^2}{n v_d} \sum_{(hkl)} \frac{m_{hkl} f_{hkl}^2}{q_{hkl}^{d-1}} L_{hkl}(q) \qquad (5)$$

where n is the number of particle per unit cell, v_d is the volume of the d-dimensional unit cell, f_{hkl} is the unit-cell structure factor, m_{hkl} is the peak multiplicity, and $L_{hkl}(q)$ is a normalized peak-shape function. The summation is over all sets of reflections hkl. Available peak shapes are Lorentzian function. The cylindrical microdomains with radius R and length L was used as $P(q)$

$$P(q) = \int_0^{\pi/2} \left[\frac{2B_1(qR\sin a)}{qR\sin a} \frac{\sin(qR\cos a / 2)}{qR\cos a / 2} \right]^2 \sin a \, da \qquad (6)$$

where $B_1(x)$ is the first order Bessel function, and a is the angle between the axis of the cylinder and the q-vector. The size distribution of $P(q)$ was modeled using Schultz-Zimm distribution. The SAXS profile obtained from experiment and theoretical curve are shown in Fig. 2. Vertical solid lines indicate the peak-position of OBDD listed in table 1. Thick arrow indicates the peak of form factor. It can be seen in Fig. 2 that the calculated SAXS curve was in excellent agreement with experimental one. The diffraction peak positions of $Pn3m$ symmetry and the corresponding scattering intensity, including weaker intensity from fifth (2) and sixth (2.12) peak, could be identified with higher accuracy.
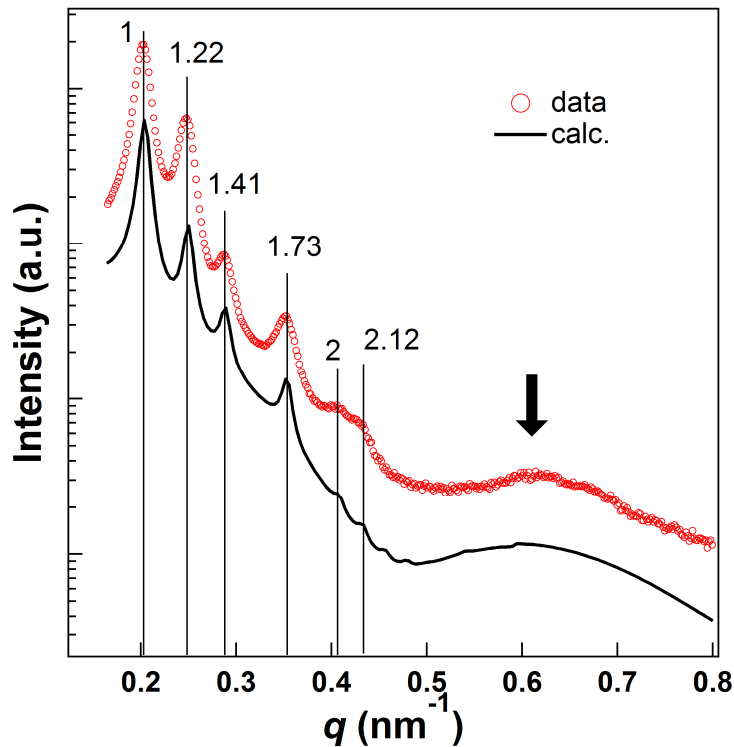
Fig. 2. SAXS profile of PS-PI / PI blend measured at 120 °C and calculated SAXS curve of OBDD structure. Vertical solid lines indicate the peak-position of OBDD listed in Table 2. Thick arrow indicates the form factor peak.

Moreover, it was reported that the lattice parameter ratio takes the value of $a(G) / a(D) = 1.576$ during transformation of Gyr to OBDD [21]. The value of $a(G) / a(D)$ was obtained to be 1.609 in this study, which was almost coincident with the early reported work. In conclusion, therefore, the OBDD microdomain was observed in our sample.

Here, let us discuss why OBDD was observed in block copolymer and homopolymer blends. It is well known that there are two types of mixing state in block copolymer / homopolymer blends [18,19]. In a wet brush state, low molecular weight homopolymers tend to be selectively uniformly solubilized into the corresponding block copolymer microdomains. On the other hand, in a dry brush state, added homopolymers tend still to be solubilized selectively into the corresponding microdomains but to localize in the middle of it. The "wet brush" or "dry brush" conditions can be controlled by the chain

length ratio (α) of homopolymer to block copolymer. Under the dry brush condition, homopolymers that is added to minority domains can fill space in the center of the domains. Thus, the added homopolymers can relieve higher packing frustration inside 4-fold nodes and lead to stabilize OBDD since minority block chains no longer have to stretch excessively to fill the centers of nodes.

As shown in Fig. 1, when the sample was heated to 160 °C, an additional new scattering peak near the high q side of the first order peak was observed. When the temperature reached at 180 °C, this additional peak was sharper and scatterings from the OBDD were not observed completely. The relative peak positions from this new structure were seen at 1 : 1.15 : 1.54 : 1.62 : 1.82 : 1.92 marked by thick arrows. From table 1, a series of the peak positions were consistent with that predicted as Gyr, indicating that a phase transition from OBDD to Gyr took place around 180 °C. The top profile in Fig. 1 was obtained from temperature drop from 200 °C to 140 °C. The diffraction peaks appeared in the relative peak positions of OBDD, and the scattering from Gyr diminished at 140 °C. The Gyr structure was confirmed to transform into the OBDD completely in cooling cycle. Therefore, it was found that the transition between OBDD and Gyr was thermo-reversible.

In order to determine the order-order transition temperature (T_{OOT}), the first order peak positions obtained during heating process versus temperature was plotted in Fig. 3. In the temperature range from 128 °C to 144 °C, only OBDD was observed. When the temperature reached at 146 °C, the diffraction peaks of Gyr appeared. The first order peak of both OBDD and Gyr was observed until 168 °C, indicating that OBDD and Gyr coexisted in this temperature range. Above 170 °C, OBDD was diminished and only Gyr was observed. The reason why the coexistence of OBDD and Gyr was observed is that the system did not reach equilibrium state due to higher heating rate. The T_{OOT} is defined as the temperature at which the first order peak of Gyr was seen, and thus this blend sample showed T_{OOT} = 146 °C.
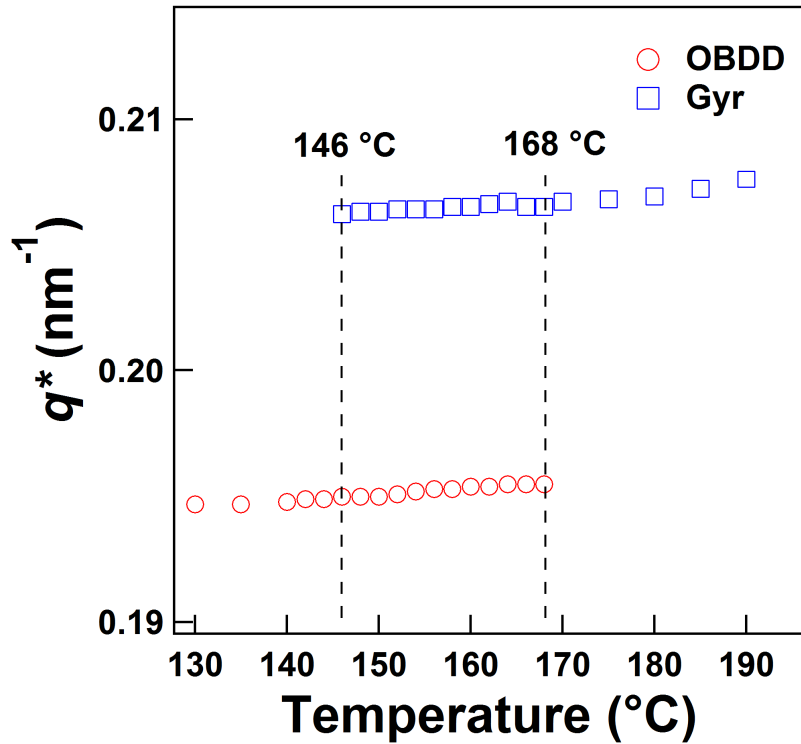
Fig. 3. The first order peak position q^* measured by SAXS as a function of T during heating process.

In order to investigate kinetically transformation between OBDD and Gyr, the time-resolved SAXS measurement after temperature jump was conducted. The sample was heated from 130 °C (OBDD) to 160 °C (Gyr) at a heating rate of 100 °C / min, and then the scattering data was accumulated just after reaching the targeted temperature. The time evolution of SAXS profiles is shown in Fig. 4 (a). Vertical solid and dashed line indicate the first order peak-position of Gyr and OBDD, respectively. After 10 sec, an additional scattering shoulder near the high q side of the first order peak was observed although the SAXS profile mainly shows the diffraction peaks of OBDD as marked thin arrows. As the duration increases, the peaks from the OBDD gradually disappeared. Simultaneously, another set of peaks appeared. After 40 sec, the relative q-peak positions were clearly seen at 1 : 1.16 : 1.54 : 1.64 : 1.84 : 1.93, indicating that OBDD transformed into Gyr. After 600 sec, the first order peak of OBDD was hardly seen in the SAXS profile. Fig. 4 (b) shows time evolution of SAXS profiles inversely from Gyr to OBDD following a temperature drop from 180 °C to 140 °C. The new shoulder near the low q

side of first order peak of Gyr emerged in the SAXS profile of 10 sec and then the intensity of this additional peak increased with passing time. The diffraction peaks corresponding to OBDD were clearly seen after 150 sec. After 1200 sec, only the diffractions of OBDD were observed, indicating that most of Gyr transformed into OBDD. Here, it was reported that two different intermediate structures were observed in the lipid system 2:1 lauric acid/dilauroyl phosphatidylcholine (2LA/DLPC) hydrated to 50 wt % H_2O using the pressure-jump technique [21]. However, in block copolymer / homopolymer blends, no diffractive intermediate phases were observed during the transformation between OBDD and Gyr.
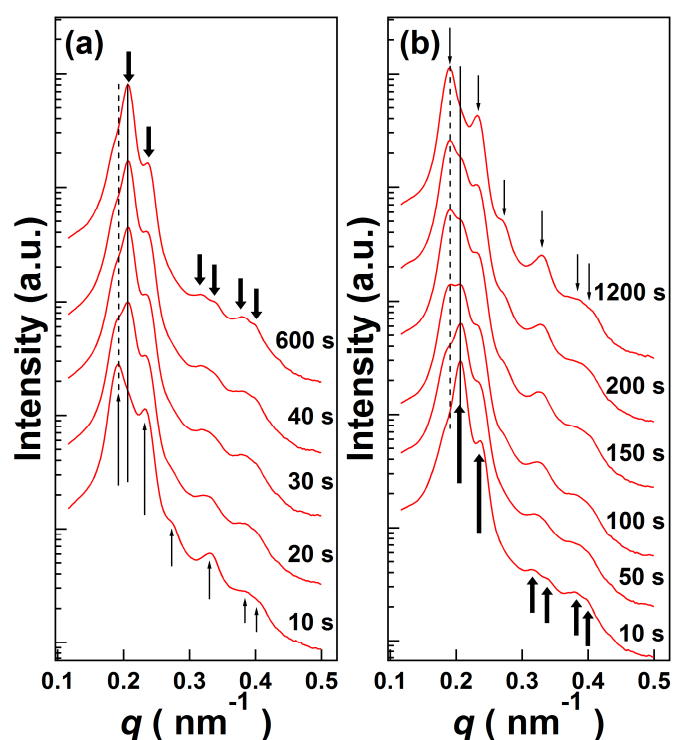

Fig. 4. Time evolution of SAXS profiles showing (a) from OBDD to Gyr following a temperature jump from 130 ℃ to 160 ℃ and (b) from Gyr to OBDD following a temperature jump drop 180 ℃ to 140 ℃. Thin arrows show scattering from OBDD, and thick arrows represent scattering peaks from Gyr. Vertical solid and dashed line indicate the first order peak-position of Gyr and OBDD, respectively.

To quantify the rate at which the transition proceeds, we evaluated changes in the amount of the disappearing of phases. The intensities of the first order peak were used for estimation of changes in the

relative amount of the two phases. The data were analyzed by using a single-exponential curve,

$$I(q) = I_\infty \cdot e^{(-t/\tau)} \qquad (7)$$

Here, t is time, and τ is the time at which the intensity is equal to $I_\infty \cdot e^{-1}$ as the characteristic time over which the transformation occurs. Fig. 5 shows the normalized peak intensity as a function of time for transition from (a) OBDD to Gyr and (b) Gyr to OBDD, respectively. The data points in Fig. 5 represent the normalized peak intensity of emergent (a) Gyr and (b) OBDD phase, respectively. The intensities were normalized with respect to those at $t = \infty$. The temperature quench or jump depth is defined as $\Delta T = \left| T_{t\arg et} \cdot T_{OOT} \right|$. The best-fit curves using eq. (7) are also shown as solid ones in Fig. 5. It was seen in Fig. 5 that the data for both transition from OBDD to Gyr and Gyr to OBDD were in almost good agreement with single-exponential curves. Here, we investigated the first-order rate (k) constant for the transformation which is defined as the reciprocal of τ. From analysis of Fig. 5, k of the transition from OBDD to Gyr was obtained as 0.056 at 160 °C ($\Delta T = 16$) and 0.143 at 170 °C ($\Delta T = 24$). On the other hand, the transition from Gyr to OBDD showed $k = 0.01$ at 130 °C ($\Delta T = 6$) and $k = 0.018$ at 120 °C ($\Delta T = 16$). It was reported that the rate of OOT was strongly influenced by quench and jump depth [23]. In this study, the rate of transition between OBDD and Gyr was found to become faster with increasing ΔT. As compared to the rate constants between 120 °C (Gyr to OBDD) and 160 °C (OBDD to Gyr) in which ΔT is almost same value, the transition from OBDD to Gyr progressed at a faster rate than that from Gyr to OBDD. In other words, our results indicate that a 3-fold node in Gyr unit cell is easily transformed from a 4-fold node. This result was almost coincident with early work in which the transition rate from OBDD to Gyr was faster than inverse transition in mixtures of 1-monoolein in 30 wt % water [24]. It is well known that the packing frustration of a 4-fold node is higher than that of a 3-fold node. To reduce the packing frustration of a 4-fold node, blended homopolymers must be distributed appropriately inside a node. Thus, the transition from Gyr to OBDD may require much time.
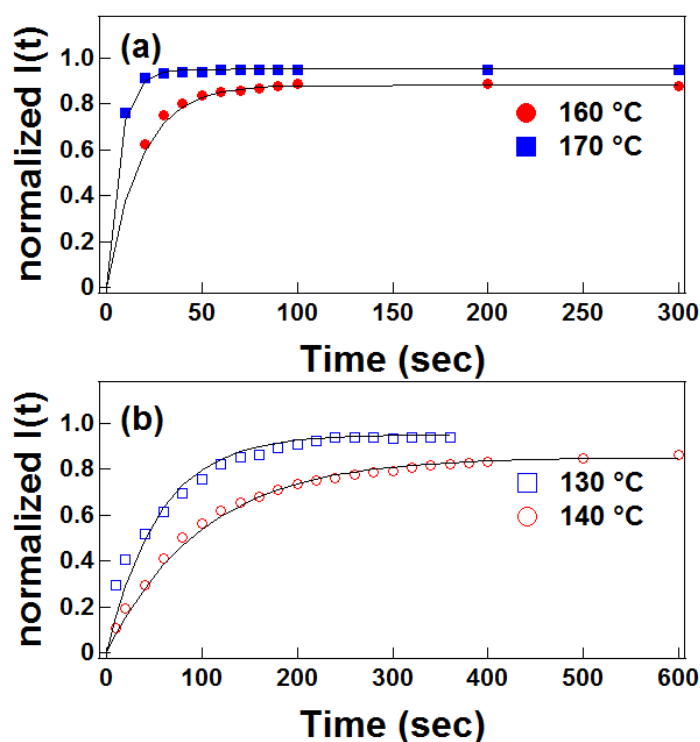
Fig. 5. Normalized integrated peak intensity as a function of time for (a) transition from OBDD to Gyr and (b) transition from Gyr to OBDD. Solid lines are best fit based on eq. (7). The data points represent the normalized peak intensity of emergent (a) Gyr and (b) OBDD phase, respectively.

CONCLUSIONS

The morphologies of the binary mixtures of PS-PI whose number-average molecular weight M_n was 38,400 g / mol and volume fraction of PI f_{PI} was 0.33 and PI having M_n = 11,400 were investigated using SAXS technique. The weight fraction of added homopolymer was 0.17. It was found that the diffraction peaks obtained experimentally were identified in predicted peak positions of OBDD. The calculated SAXS curve for OBDD was in excellent agreement with experimental one. Besides, since the lattice parameter ratio was $a(G) / a(D) = 1.609$ in this study. Thus, we conclude that the OBDD structure was actually observed in block copolymer / homopolymer blends. The key of appearance of OBDD phase is the dry brush condition of added homopolymers. Under the dry brush state, added homopolymers localize in the center of 4-fold nodes, leading to stabilize OBDD microdomains due to

14

relieving higher packing frustration inside nodes. When the sample was heated above 146 °C, OBDD changed to Gyr. The kinetics of the transformation between OBDD and Gyr was also investigated using time-resolved SAXS experiments. The intermediate structure during the transition between OBDD and Gyr was not observed in block copolymer / homopolymer blend system. A comparison between the rates of transformation revealed that the rate of the OBDD to Gyr transformation was faster than that of the Gyr to OBDD. This was because blended homopolymers must be re-distributed appropriately inside 4-fold nodes having higher packing frustration, when the transition proceeded from Gyr to OBDD. Therefore, the transition from Gyr to OBDD may require much time.

We have discovered OBDD structure in present PS-PI/PI blend system (normal amorphous polymer) that was different series of polymer system that was sPP-PS and sPP-PS / PS blend system [5] (a slightly specific polymer for chain conformation). The discovery of those stable OBDD structures ensures universality of the existence of OBDD structure in block copolymer / homopolymer system in dry state.

ACKNOWLEDGMENT

REFERENCE

[1] MEULER ADAM J, HILLMYER MARC A, BATES FRANK S, *Macromolecules*, 42 (2009) 7221.

[2] LEE JAE-HWANG, KOH CHEONG Y, SINGER JONATHAN P, JEON SEOG-JIN, MALDOVAN MARTIN, STREIN ORI, THMAS EDWIN L, *Adv. Mater.*, 26 (2014) 532.

[3] HAJUDUK DAMIAN A, HARPER PAUL E, GRUNER SOL M, HONEKER CHRISTIAN C, KIM GIA, THOMAS EDWIN L,FETTERS LEWIS J, *Macromolecules*, 27 (1994) 4063.

[4] TAKENAKA MIKIHITO, WAKADA TSUTOMU, AKASAKA SATOSHI, NISHITSUJI SHOTARO, SAIJO KENJI, SHIMIZU HIROFUMI, KIM MYUNG I, HASEGAWA HIROKAZU, *Macromolecules*, 40 (2007) 4399.

[5] CHU CHE-YI, LIN WEN-FU, TSAI JING-CHERNG, LAI CHIA-SHENG, LO SHEN-CHUAN, CHEN HSIN-LUNG, HASHIMOTO TAKEJI, *Macromolecules*, 45 (2012) 2471.

[6] THOMAS EDWIN L, ALWARD DAVID B, KINNING DAVID J, MARTIN DAVID C, HANDLIN DALE L, FETTERS LEWIS J, *Macromolecules*, 19 (1986) 2197.

[7] WINEY KAREN I, THOMAS EDWIN L, FETTERS LEWIS J, *Macromolecules*, 25 (1992) 422.

[8] HASEGAWA HIROKAZU, TANAKA HIDEAKI, YAMASAKI KOMEI, HASHIMOTO TAKEJI, *Macromolecules*, 20 (1987) 1651.

[9] MATSEN MARK W, SCHICK M, *Macromolecules*, 27 (1994) 6761.

[10] MATSEN MARK W, BATES FRANK S, *Macromolecules*, 29 (1996) 1091.

[11] HAJDUK DAMIAN A, KARPER PAUL E, GRUNER SOL M, HONEKER CHISTIAN C, KIM GIA, THOMAS EDWIN L, FETTERS LEWIS J, *Macromolecules*, 27 (1994) 4063.

[12] MATSEN MARK W, *Phys. Rev. Lett.*, 74 (1995) 4225.

[13] MAREAU VINCENT H, AKASAKA SATOSHI, OSAKA TAKETSUGU, HASEGAWA HIROKAZU, *Macromolecules*, 40 (2007) 9032.

[14] HAJDUK DAMIAN A, HARPER PAUL E, GRUNER SOL M, HONEKER CHRISTIAN C, THOMAS EDWIN L, FETTERS LEWIS J, *Macromolecules*, 28 (1995) 2570.

[15] MARTINEZ-VERACOECHEA FRANCISCO J, ESCOBEDO FERNANDO A, *Macromolecules*, 38 (2005) 8522.

[16] MARTINEZ-VERACOECHEA FRANCISCO J, ESCOBEDO FERNANDO A, *J. Chem. Phys* , 125 (2006) 104907-1.

[17] MATSEN MARK W, *Macromolecules*, 28 (1995) 5765.

[18] MARTINEZ-VERACOECHEA FRANCISCO J, ESCOBEDO FERNANDO A, *Macromolecules*,

42 (2009) 9058.

[19] KHANDPUR ASHISH K, FORSTER STEPHAN, BATES FRANK S, HAMLEY IAN W, RYAN ANTHONY J, BRAS WIM, ALMDAL KRISTOFFER, MORTENSEN KELL, *Macromolecules*, 28 (1995) 8796.

[20] FORSTER A, TIMMANN A, KONARAD M, SCHELLBACH C, MEYER A, FUNARI SS, MULYANEY P, KNOTT R, *J. Phys. Chem. B*, 109 (2005) 1347.

[21] SQUIRES ADAM M, TEMPLER R H, SEDDON J M, WOENKHAUS J, WINTER R, NARAYANAN T, FINET S, *Phys. Rev. E*, 72 (2005) 011502-1.

[22] SEMENOV AN, *Macromolecules*, 26 (1993) 2273.

[23] LAI CHIAJEN, LOO YUEH-LIN, REGISTER RICHARD A, *Macromolecules*, 38 (2005) 7098.

[24] CONN CHARLOTTE E, CES OSCAR, SQUIRES ADAM M, MULET XAVIER, WINTER ROLAND, FINET STEPHANIE M, TEMPLER RICHARD H, SEDDON JOHN M, *Langmuir*, 24 (2008) 2331.

Table and Figure captions.

Fig. 1. SAXS profiles of PS-PI / PI blend during heating process. SAXS profile after cooling from 200 °C to 140 °C is also shown (top profile). Thin arrows show scattering from OBDD, and thick arrows represent scattering peaks from Gyr.

Fig. 2. SAXS profile of PS-PI / PI blend measured at 120 °C and calculated SAXS curve of OBDD structure. Vertical solid lines indicate the peak-position of OBDD listed in Table 2. Thick arrow indicates the form factor peak.

Fig. 3. The first order peak position q^* measured by SAXS as a function of T during heating process.

Fig. 4. Time evolution of SAXS profiles showing (a) from OBDD to Gyr following a temperature jump from 130 °C to 160 °C and (b) from Gyr to OBDD following a temperature jump drop 180 °C to 140 °C. Thin arrows show scattering from OBDD, and thick arrows represent scattering peaks from Gyr. Vertical solid and dashed line indicate the first order peak-position of Gyr and OBDD, respectively.

Fig. 5. Normalized integrated peak intensity as a function of time for (a) transition from OBDD to Gyr and (b) transition from Gyr to OBDD. Solid lines are best fit based on eq. (7). The data points represent the normalized peak intensity of emergent (a) Gyr and (b) OBDD phase, respectively.

Table 1. Calculated relative peak positions of OBDD, Gyr, *Fddd* and observed relative peak positions.